A Hybrid Controller for Boost Inverter: Modeling, Simulation, and Experimental Results

Anwar Muqorobin[1], Tri Desmana Rachmildha[2], Yanuarsyah Haroen[2], and Estiko Rijanto[1]

[1]Research Center for Electrical Power and Mechatronics, Indonesian Institute of Sciences
Jl. Sangkuriang, Bandung 40135, INDONESIA
[2]School of Electrical Engineering and Informatics, Institut Teknologi Bandung
Jl. Ganesha 10, Bandung 40132, INDONESIA
anwa006@lipi.go.id

Abstract: Some controls have been introduced to control boost inverter, e.g. linear control, sliding mode control, and energy shaping based control. In this paper, the authors propose boost inverter control based on hybrid model. It is easier to design because it does not require complex mathematical formula. Simulations and experiments have been conducted to determine the performance of the proposed control under steady state and during transient state with a variety of load, inductance, and capacitance. The simulation and experimental results show that the hybrid control can work properly.

Keywords: Boost inverter, hybrid model, and control.

1. Introduction

Inverters are widely used in various applications such as uninterruptible power supply (UPS), motor drive, and utility interface. Buck inverter is commonly used to obtain an AC output from a DC source. One characteristic of this inverter is that the output voltage is lower than the DC input voltage. If the required voltage is greater than the input, a dc-dc boost converter must be added in the front of inverter [1]. The addition of dc-dc boost converter on buck inverter can increase the volume, weight, price, and losses.

To avoid that, it is necessary to use boost inverter. Boost inverter can be made of two dc-dc boost converters with load placed on each output of the dc-dc boost converter [2]. Compared to buck inverter equipped with a dc-dc boost converter, boost inverter circuit requires less switching components. Boost inverter can generate voltage that is greater or smaller than the input voltage. As a result, this inverter is more suitable to generate variable AC voltage with a wide range of amplitude variation.

The control that is used in [2] is a sliding mode control. There are two controls for each dc-dc boost converter. The sliding surface is formed by the inductor current error and output voltage error. Inductor current error is obtained from the inductor current passed to a high pass filter. The filter cut-off frequency is below the switching frequency in order to pass the switching ripple effect. To avoid chattering phenomena, the authors used a hysteresis in the sliding surface. The principle of current mode control for boost inverter was proposed in [3]. The authors compared the proposed control with sliding mode control. Experiments have been conducted in the condition of input voltage variaton and short circuit. The experimental results showed that the sliding mode control cannot work properly when the input voltage changed and produces large transient currents during a short circuit. On the other hand, the control proposed in [3] could work well under those two conditions. A control method based on small-signal analysis has been introduced in [4]. The advantage of the control is that it only need a voltage sensor. The system is modeled by using a small signal model around the duty cycle of 0.5. Simulation results showed that the proposed control could work well when the input voltage changed. Energy shaping control also has been published [5]. However, this control uses a very complicated mathematical formula. The other sliding mode control was proposed in [6] to control both dc-dc converters simultaneously. Unlike some boost inverter controls that have been mentioned before, the proposed control only use a controller. The sliding surface consists of PI (Proportional and

Received: December 11st, 2020. Accepted: March 29th, 2021
DOI: 10.15676/ijeei.2021.13.1.10

Integral) control of boost inverter output voltage error and inductor current error from both dc-dc boost converters. Simulation results showed that the voltage of each dc-dc converter is not sinusoidal, but the boost inverter output voltage is sinusoidal indeed. The other controls e.g. one cycle control and resonant controllers also have been proposed for boost inverter [7][8].

In this paper, the authors propose a hybrid model-based control to control the boost inverter. Compared to the boost inverter controls that have been proposed by previous researchers, this control is easier to design because it does not require complex mathematical formulas. Simulations and experiments were conducted to verify the performance of the proposed control.

2. Boost Inverter Hybrid Modeling

A hybrid model is a mathematical model that represents complex systems with a hierarchical structure and may consist of continuous and discrete subsystems that interact with each other. The evolution of discrete subsystem depends on the continuous information and the evolution of the continuous subsystem depends on the discrete information. A hybrid system is expressed by $H = (Q, X, f, I, E, G)$, where $Q = \{q_1, \dots q_n\}$ is a set of discrete states, $X \subseteq R^n$ is continuous state spaces, $f: Q \rightarrow (X \rightarrow R^n)$ assign every discrete state to a Lipschitz continuous vector field on X, i.e. the dynamic equation $\dot{x} = f(x, t)$, $I: Q \rightarrow 2^x$ assign each $q \in Q$ an invariant set, $E \subseteq Q\ x\ Q$ is a collection of discrete transitions, and $G: E \rightarrow 2^x$ is guard equation for each $e = (q, q') \in E$.

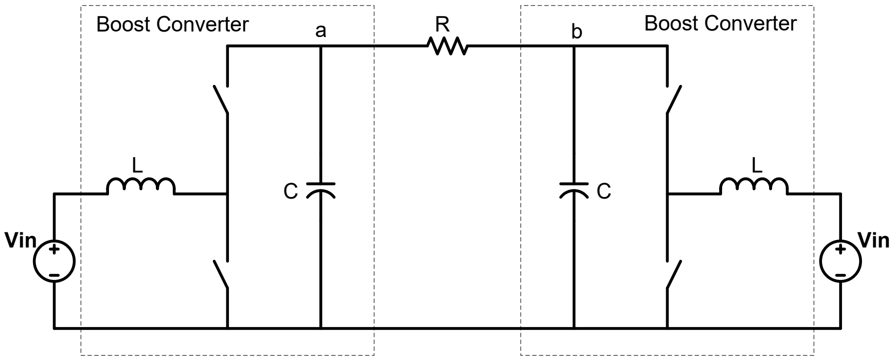

Figure 1. Boost inverter.

Power electronics circuit is one of hybrid system. The continuous state is the current and voltage of passive components such as capacitor and inductor. The discrete state is generated by the switching components such as MOSFET, IGBT, and diode. The control for power electronics hybrid model is guards that determine the transition of a discrete state to another discrete state, to obtain the desired continuous subsystem response [9].

The boost inverter topology in this study is shown in Figure. 1. The inverter consists of two dc-dc boost converters. The boost inverter model is shown in Figure. 2. The set of discrete state is $Q = \{q_1, q_2, q_3, q_4\}$ as shown in Figure. 3. There are four continuous states, i.e. $x = \{i_{La}, v_{oa}, i_{Lb}, v_{ob}\}$, where i_{La} is the inductor current of the first boost converter, v_{oa} is the output voltage of the first boost converter, i_{Lb} is the inductor current of the second boost converter, and v_{ob} is the output voltage of the second boost converter,

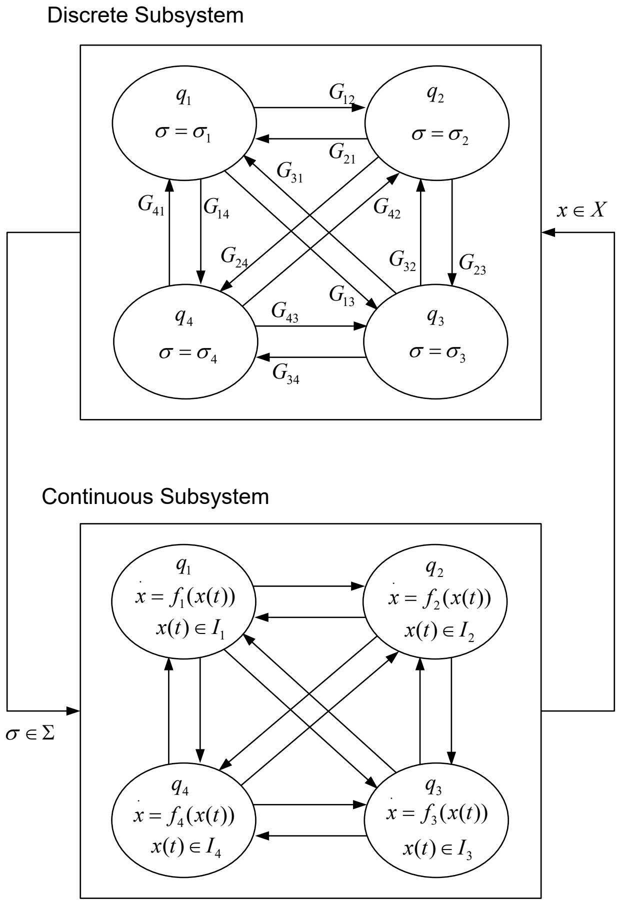

Figure 2. Boost inverter hybrid model

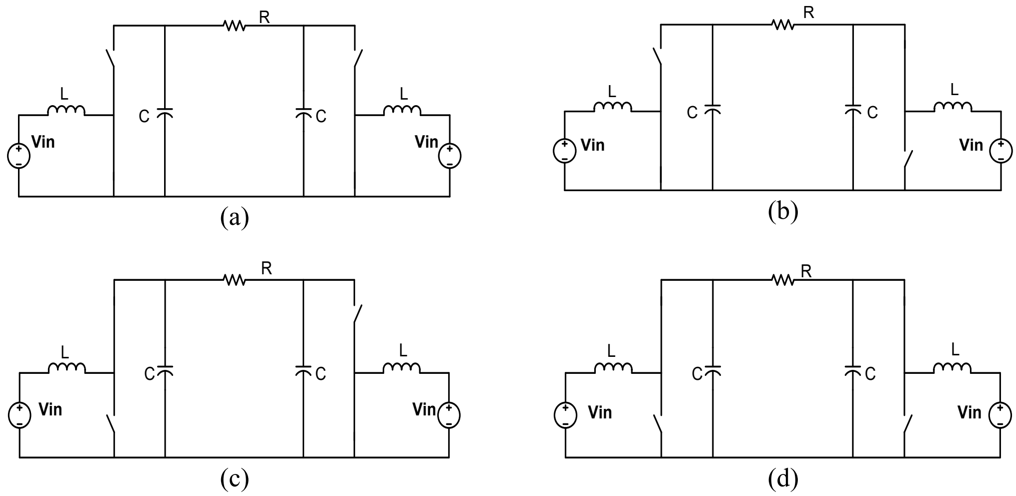

Figure 3. The discrete state of boost inverter (a) $Q = q_1$, (b) $Q = q_2$, (c) $Q = q_3$, and (d) $Q = q_4$

The Lipshitz vector field f_i for $Q = q_1$, $Q = q_2$, $Q = q_3$, and $Q = q_4$, each is shown in (1), (2), (3), and (4) respectively.

$$\dot{x} = f_1 = \begin{bmatrix} 0 & 0 & 0 & 0 \\ 0 & -\frac{1}{RC} & 0 & \frac{1}{RC} \\ 0 & 0 & 0 & 0 \\ 0 & \frac{1}{RC} & 0 & -\frac{1}{RC} \end{bmatrix} x + \begin{bmatrix} \frac{V_{in}}{L} \\ 0 \\ \frac{V_{in}}{L} \\ 0 \end{bmatrix} \quad (1)$$

$$\dot{x} = f_2 = \begin{bmatrix} 0 & 0 & 0 & 0 \\ 0 & -\frac{1}{RC} & 0 & \frac{1}{RC} \\ 0 & 0 & 0 & -\frac{1}{L} \\ 0 & \frac{1}{RC} & \frac{1}{C} & -\frac{1}{RC} \end{bmatrix} x + \begin{bmatrix} \frac{V_{in}}{L} \\ 0 \\ \frac{V_{in}}{L} \\ 0 \end{bmatrix} \quad (2)$$

$$\dot{x} = f_3 = \begin{bmatrix} 0 & -\frac{1}{L} & 0 & 0 \\ \frac{1}{C} & -\frac{1}{RC} & 0 & \frac{1}{RC} \\ 0 & 0 & 0 & 0 \\ 0 & \frac{1}{RC} & 0 & -\frac{1}{RC} \end{bmatrix} x + \begin{bmatrix} \frac{V_{in}}{L} \\ 0 \\ \frac{V_{in}}{L} \\ 0 \end{bmatrix} \quad (3)$$

$$\dot{x} = f_4 = \begin{bmatrix} 0 & -\frac{1}{L} & 0 & 0 \\ \frac{1}{C} & -\frac{1}{RC} & 0 & \frac{1}{RC} \\ 0 & 0 & 0 & -\frac{1}{L} \\ 0 & \frac{1}{RC} & \frac{1}{C} & -\frac{1}{RC} \end{bmatrix} x + \begin{bmatrix} \frac{V_{in}}{L} \\ 0 \\ \frac{V_{in}}{L} \\ 0 \end{bmatrix} \quad (4)$$

In (1)-(4), L is the inductance, C is the capacitance, R is the load resistance, and V_{in} is the input voltage.

The set of discrete transition is

$$E = \begin{Bmatrix} (q_1, q_2)(q_1, q_3)(q_1, q_4)(q_2, q_1)(q_2, q_3)(q_2, q_4) \\ (q_3, q_1)(q_3, q_2)(q_3, q_4)(q_4, q_1)(q_4, q_2)(q_4, q_3) \end{Bmatrix} \quad (5)$$

The guard equations for the boost inverter are as follow

$$G(q_2, q_1) = \{x \in R^4 | \ \sigma = \sigma_1\} \quad (6)$$
$$G(q_3, q_1) = \{x \in R^4 | \ \sigma = \sigma_1\} \quad (7)$$
$$G(q_4, q_1) = \{x \in R^4 | \ \sigma = \sigma_1\} \quad (8)$$
$$G(q_1, q_2) = \{x \in R^4 | \ \sigma = \sigma_2\} \quad (9)$$
$$G(q_3, q_2) = \{x \in R^4 | \ \sigma = \sigma_2\} \quad (10)$$
$$G(q_4, q_2) = \{x \in R^4 | \ \sigma = \sigma_2\} \quad (11)$$
$$G(q_1, q_3) = \{x \in R^4 | \ \sigma = \sigma_3\} \quad (12)$$
$$G(q_2, q_3) = \{x \in R^4 | \ \sigma = \sigma_3\} \quad (13)$$
$$G(q_4, q_3) = \{x \in R^4 | \ \sigma = \sigma_3\} \quad (14)$$
$$G(q_1, q_4) = \{x \in R^4 | \ \sigma = \sigma_4\} \quad (15)$$
$$G(q_2, q_4) = \{x \in R^4 | \ \sigma = \sigma_4\} \quad (16)$$
$$G(q_3, q_4) = \{x \in R^4 | \ \sigma = \sigma_4\} \quad (17)$$

The σ_i are defined in the next section.

3. Boost Inverter Control

To control the boost inverter, each dc-dc converter must produce a unipolar sinusoidally dc-biased voltage. To maximize the voltage deviation at the load, the following references are used.

$$v_{oaref} = V_{dc} + \frac{V_r}{2}\sin(\omega t) \tag{18}$$

$$v_{obref} = V_{dc} - \frac{V_r}{2}\sin(\omega t) \tag{19}$$

Where v_{oaref} is the output voltage reference of the first boost converter, v_{obref} is the ouput voltage reference of the second boost converter, and V_r is amplitude of the boost inverter reference. The value of V_{dc} can be chosen arbitrary, but it must fulfill the following requirements.

$$V_{dc} \geq v_{in} + \frac{V_r}{2} \tag{20}$$

The overall control is shown in Figure. 4. The hybrid control block is fed by the states $x = \{i_{La}, v_{oa}, i_{Lb}, v_{ob}\}$ and the references $x_d = \{i_{Laref}, v_{oaref}, i_{Lbref}, v_{obref}\}$. The PI controls are used to produce the current references. There are two PI controls, each is fed by an error between the voltage reference v_{oaref} and v_{obref} and the output voltage v_{oa} and v_{ob}.

The hybrid control minimizes the cosine between $x - x_d$ and $f_i(x)$ by using the following algorithm [10]-[12].

$$\sigma_i = arg \min_{i \in \Lambda} \frac{\langle x - x_d, f_i(x) \rangle}{\|x - x_d\| \, \|f_i(x)\|} \tag{21}$$

Where $e = x - x_d$. Since $\|x - x_d\|$ does not depend on i, it is ignored in the control computation. By selecting the minimum value of cosine between the vectors $f(x)$ and $e = x - x_d$, it will make x closer to the desired x_d. The pseudo-code of the control algorithm is shown in Figure. 5.

4. Simulation Results

PSIM simulations were conducted by using boost inverter parameters as shown in Table 1. The voltage references of the boost converters are

$$v_{oaref} = 320 + 156\sin(100\pi t) \tag{22}$$

$$v_{obref} = 320 - 156\sin(100\pi t) \tag{23}$$

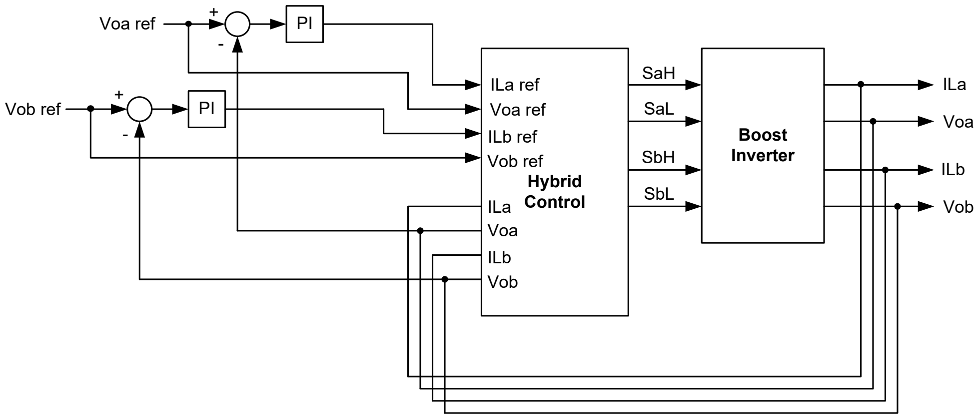

Figure 4. Block diagram of boost inverter control

```
// Sa = 0;  Sb = 0;
f1a1 = vin/L;
f2a1 = -(voa - vob)/(R*C);
f1b1 = vin/L;
f2b1 = (voa - vob)/(R*C);
f1mag = sqrt(f1a1*f1a1 + f2a1*f2a1 + f1b1*f1b1 + f2b1*f2b1);

// Sa = 0;  Sb = 1;
f1a2 = vin/L;
f2a2 = -(voa - vob)/(R*C);
f1b2 = (vin - vob)/L;
f2b2 = (voa - vob)/(R*C) + iLb/C;
f2mag = sqrt(f1a2*f1a2 + f2a2*f2a2 + f1b2*f1b2 + f2b2*f2b2);

// Sa = 1;  Sb = 0;
f1a3 = (vin - voa)/L;
f2a3 = -(voa - vob)/(R*C) + iLa/C;
f1b3 = vin/L;
f2b3 = (voa - vob)/(R*C);
f3mag = sqrt(f1a3*f1a3 + f2a3*f2a3 + f1b3*f1b3 + f2b3*f2b3);

// Sa = 1;  Sb = 1;
f1a4 = (vin - voa)/L;
f2a4 = -(voa - vob)/(R*C) + iLa/C;
f1b4 = (vin - vob)/L;
f2b4 = (voa - vob)/(R*C) + iLb/C;
f4mag = sqrt(f1a4*f1a4 + f2a4*f2a4 + f1b4*f1b4 + f2b4*f2b4);

deltaia = iLa -  iLaref;
deltaib = iLb -  iLbref;
deltava = voa -  voaref;
deltavb = vob -  vobref;

delta1 = (deltaia*f1a1 + deltava*f2a1 + deltaib*f1b1 +deltavb*f2b1)/f1mag;
delta2 = (deltaia*f1a2 + deltava*f2a2 + deltaib*f1b2 +deltavb*f2b2)/f2mag;
delta3 = (deltaia*f1a3 + deltava*f2a3 + deltaib*f1b3 +deltavb*f2b3)/f3mag;
delta4 = (deltaia*f1a4 + deltava*f2a4 + deltaib*f1b4 +deltavb*f2b4)/f4mag;

Sa = 0; Sb = 0;
if (delta1<delta2 && delta1<delta3 && delta1<delta4)
   {
   Sa = 0;
   Sb = 0;
   }
if (delta2<delta1 && delta2<delta3 && delta2<delta4)
   {
   Sa = 0;
   Sb = 1;
   }
if (delta3<delta1 && delta3<delta2 && delta3<delta4)
   {
   Sa = 1;
   Sb = 0;
   }
if (delta4<delta1 && delta4<delta2 && delta4<delta3)
   {
   Sa = 1;
   Sb = 1;
        }
```

Figure 5. Pseudo-code of hybrid control

Table 1. Boost inverter parameters

Parameters	Values
Input voltage	150 V
Output voltage amplitude	312 V
Output fundamental frequency	50 Hz
Inductor	150 uH
Capasitor	680 uF
Resistive Load	20 Ohm

In the simulation, the PI controls use Kp constant of 10 and Ti of 0.1. Simulation results under steady state are shown in Figure. 6. Simulation results using switching frequency of 20 kHz are shown in Figure. 6(a) and switching frequency of 100 kHz in Figure. 6(b). Figure. 6 shows that the boost converter output voltage is a sinusoidal with DC bias of 320 V that is greater than the input voltage. Figure. 6 also shows that the boost inverter control can achieve stable condition. Comparing Figures. 6(a) to 6(b), it can be seen that increasing the switching frequency can reduce the ripples in the inductor currents, boost converter output voltage, and boost inverter output voltage. When frequency of 20 kHz is used, the THD (Total Harmonic Distortion) of the boost inverter output voltage is 1.87%, while frequency of 100 kHz produces THD of 0.25%.

The simulation results during transient state are shown in Figure. 7. In Figure. 7, we can see two transient states, i.e. start-up from zero second and load step from 20 Ohm to 10 Ohm in 0.1 second. From Figure. 7, it is known that the steady state can be achieved in less than one fundamental period.

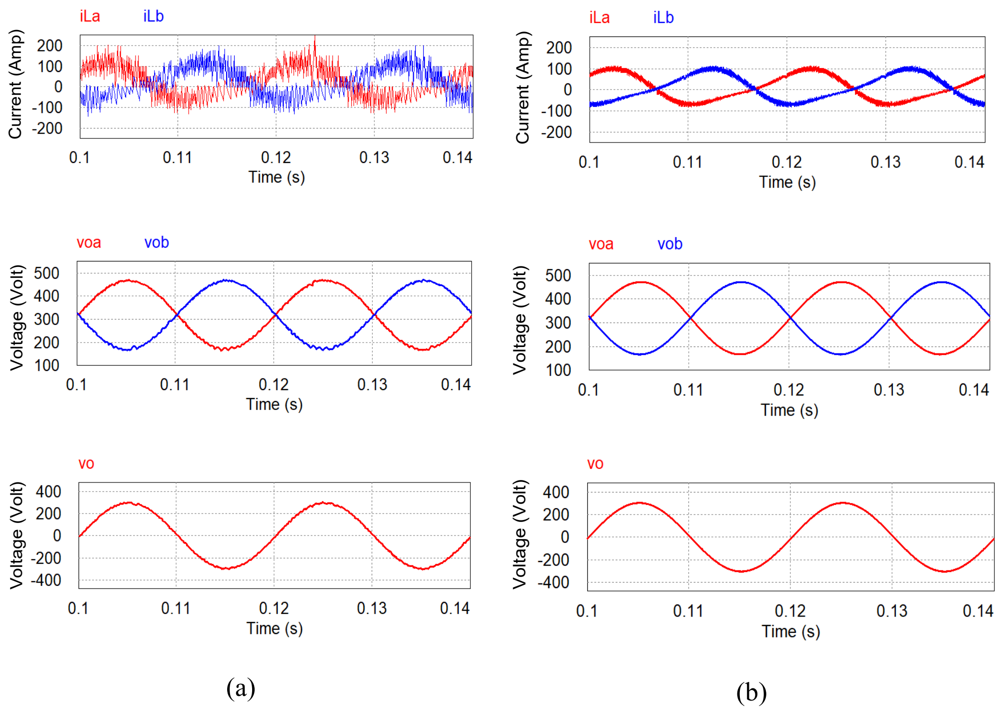

Figure 6. Simulation results during steady state (a) sampling frequency of 20 kHz (b) sampling frequency of 100 kHz

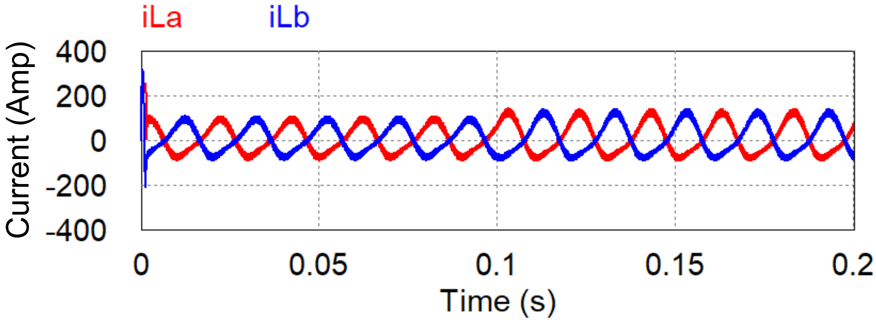

(a)

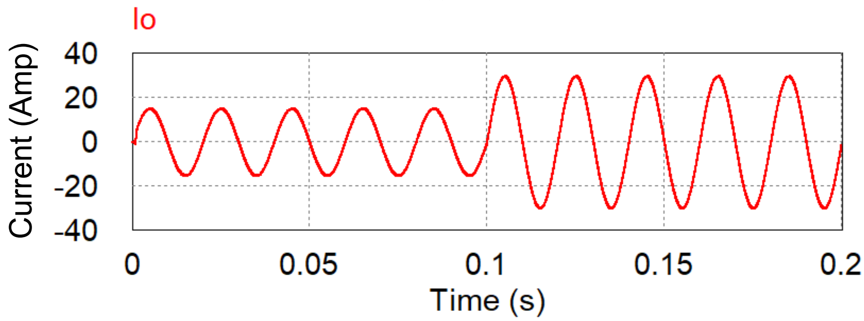

(b)

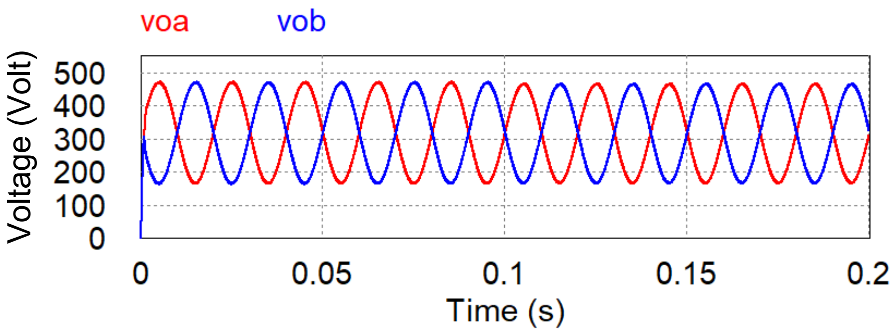

(c)

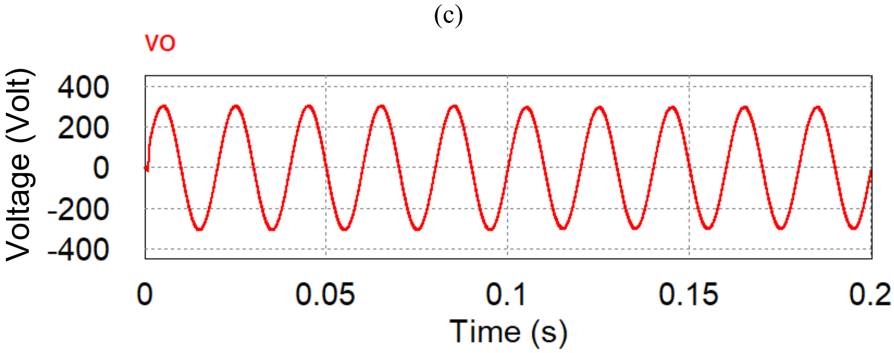

(d)

Figure 7. Simulation results with transient state (a) inductor current, (b) load current, (c) boost converter, and (d) boost inverter output voltage

5. Experimental Results

The parameters for the laboratory experiments are shown in Table 2. The PI control constants are Kp = 0.15 and Ki = 0.05. The overall control algorithm is implemented in a digital signal processor TMS28335 from Texas Instruments. The voltage references are

$$v_{oaref} = 10 + 3.5\sin(100\pi t) \quad (24)$$

$$v_{obref} = 10 - 3.5\sin(100\pi t) \quad (25)$$

Table 2. Experimental parameters

Parameters	Value
Input voltage	5 V
Output voltage amplitude	7 V
Output fundamental frequency	50 Hz
Inductor	150 uH
Capasitor	680 uF
Resistive Load	20 Ohm

The experimental results are shown in Figure. 8. Figure. 8(a) shows the inductor current of each converter dc-dc boost. As in the simulation, the inductor current ripple looks so obvious. The output voltage of each dc-dc boost converter is shown in Figure. 8(b). The waveform is not pure sinusoidal. It is similar to the results in [6]. The output voltage is shown in Figure. 8(c). The ripple that is visible on the output voltage is caused by low sampling frequency of 20 kHz. The FFT (Fast Fourier Transform) of the boost inverter output voltage is shown in Figure. 8(d). The output voltage amplitude at 50 Hz is 6.85 V and the THD is 5.33%. By using higher frequency, it is expected that the THD of boost inverter output voltage becomes lower, as shown by the simulation results.

The experiments were also conducted to verify the robustness of the hybrid control when the parameter values changed. The inductance variation experiments were conducted by varying the inductance values on the digital signal processor from 120uH to 180uH (in the range of 20% of the nominal value 150uH). On the other hand, the real inductors used in the boost inverter are remain unchanged, i.e. 150uH. The experimental results are shown in Table 3. It can be seen that the deviation value of inductance has no effect on the resulting control. The output voltage THD only change less than 1%, that is below the measurement precision.

The capacitance variation experiments were done by varying the capacitance values on digital signal processor from 544 uF to 816 uF (in the range of 20% of the nominal value of 680 uF). The capacitances that were used in the boost inverter remain unchanged, i.e. 680 uH. The experimental results are shown in Table 4. Similar to the inductance, the deviation value of the capacitance has no effect on the output voltage THD.

Table 3. Inductance variation effect

Inductance (uH)	Magnitude at 50Hz (Volt)	THD (%)
120	6.69	5.79
135	6.72	4.97
150	6.67	6.04
165	6.59	5.49
180	6.65	5.47

Table 4. Capacitance variation effect

Capacitance (uF)	Magnitude at 50Hz (Volt)	THD (%)
544	6.67	5.95
612	6.66	6.06
680	6.71	4.64
748	6.61	6.41
816	6.67	6.66

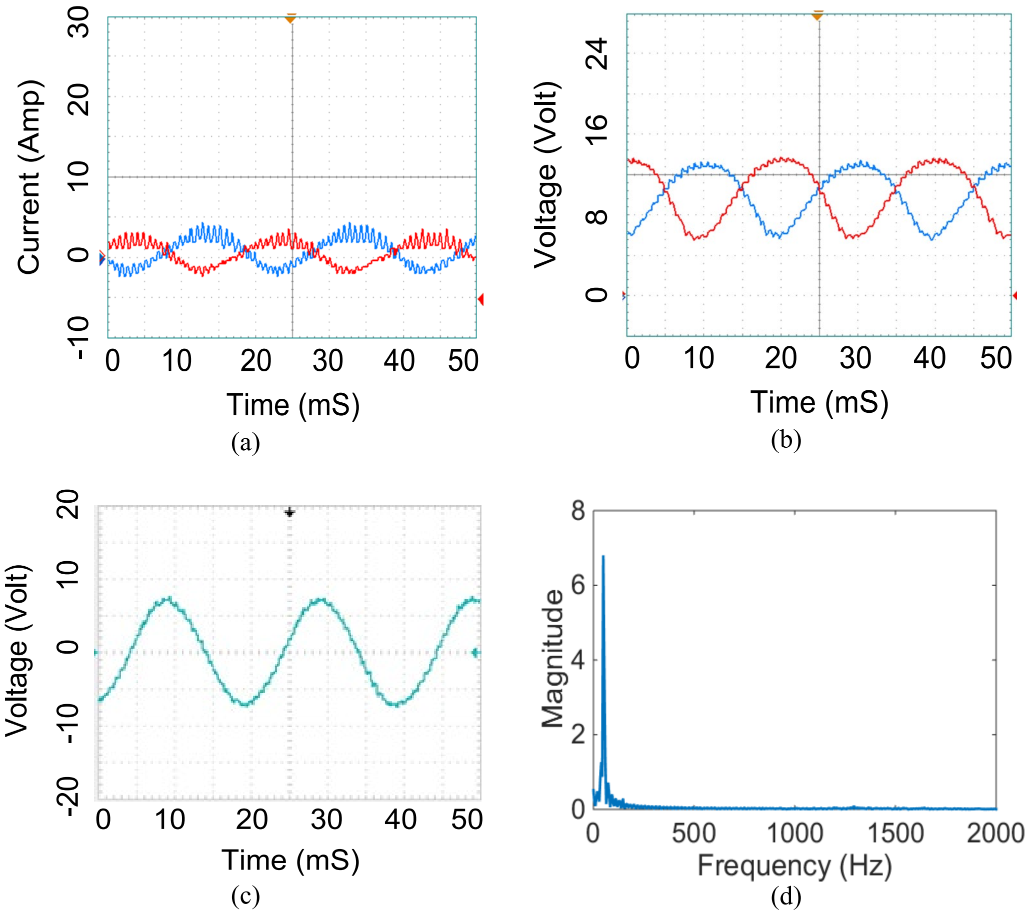

Figure 8. Boost inverter experimental results: (a) the inductor current (b) the output voltages of dc-dc boost converters, (c) the boost inverter output voltage, and (d) the spectrum of boost inverter output voltage

6. Conclusion

A hybrid control has been proposed to control a boost inverter. Simulations and experiments have been conducted to verify the performance of the boost inverter control. The simulation and experimental results show that the steady state can be achieved in less than one fundamental period. The proposed hybrid control is robust despite of load variation, inductance variation, and capacitance variation. The constraint of the hybrid control implementation is that it need long time to calculate the overall algorithm. In order to get a good response, i.e. lower THD, faster digital processor is needed.

7. Acknowledgement

Authors would like to thank **DIKTI** of **Kemenristek** (Ministry of Research and Technology) of the Republic of Indonesia for the support of the research through the scheme of Applied Research Scheme 2019-2020.

8. References

[1]. P.A. Dahono, "Derivation of high voltage-gain step-up DC-DC power converters," *International Journal on Electrical Engineering and Informatics*, vol. 11, no. 2, pp. 236-251, June 2019.
[2]. R.O. Caceres and I. Barbi, "A boost dc-ac converter: analysis, design, and experimentation," *IEEE Transactions on Power Electronics*, vol. 14, no. 1, pp. 134-141, January 1999.
[3]. P. Sanchis, A. Ursaea, E. Gubía, and L. Marroyo, "Boost dc-ac inverter: a new control strategy," *IEEE Transactions on Power Electronics*, vol. 20, no. 2, pp. 343-353, March 2005.
[4]. A.S. Khan and K.M. Rahman, "Voltage mode control of single phase boost inverter," 5th *International Conference on Electrical and Computer Engineering (ICECE)*, pp. 665-670, Dec. 2008.
[5]. Albea, F. Gordillo, and J. Aracil, "Control of the boost dc-ac converter by energy shaping," *The 32nd Annual Conference of the IEEE Industrial Electronics Society*, Paris : France, 2007.
[6]. Cortes, N. Vázquez, J. Alvarez-Gallegos, "Dynamical sliding-mode control of the boost inverter," *IEEE Transactions on Industrial Electronics*, vol. 56, no. 9, pp. 3467-3476, September 2009.
[7]. I. Purnama et al., "One cycle controlled grid-tied differential boost inverter," *IET Power Electronics*, vol. 9, no. 11, pp. 2216-2222, 2016.
[8]. S. Huang et al., "Grid-current control of differential boost inverter with hidden LCL filters," *IEEE Transactions on Power Electronics*, vol. 34, no. 1, pp. 889 - 903, January 2019.
[9]. C. Sreekumar and V. Agarwal, "A hybrid control algorithm for voltage regulation in dc-dc boost converter," *IEEE Transactions on Industrial Electronics*, vol. 55, no. 6, pp. 2530-2538, June 2008.
[10]. M. Senesky, G. Eirea, and T.J. Koo, "Hybrid modeling and control of power electronics," in Hybrid Systems: Computation & Control. Berlin, Germany: Springer-Verlag, pp. 450-465, 2003.
[11]. L. Atmopawiro, "Pemodelan hibrida pada boost inverter menggunakan matlab, simulink, dan psim (Boost inverter hybrid modeling using matlab, simulink and psim)," B.Sc. Thesis, Institute of Technology Bandung, 2011.
[12]. C. Sreekumar and V. Agarwal, "Hybrid control of a boost converter operating in discontinuous current mode," *Power Electronics Specialists Conference*, pp. 1-6, June 2006.

Anwar Muqorobin was born in Temanggung, Indonesia in 1977. He received the bachelor degree from Universitas Diponegoro in 2001, the master degree from Institut Teknologi Bandung in 2013, and the doctor degree from Institut Teknologi Bandung in 2019, all in Electrical Engineering. He is currently a researcher at Research Center for Electrical Power and Mechatronics, Indonesian Institute of Sciences (P2 Telimek LIPI). His research interest is inverter. He can be contacted at anwa006@lipi.go.id or anwa006@gmail.com

Tri Desmana Rachmildha was born in Indonesia in 1975. He received B.Eng and M.Eng degrees in electrical engineering from Bandung Institute of Technology (ITB), Indonesia, in 1998 and 2002, respectively. He received Doctor Degree in Electrical Engineering from Joint PhD Supervision Program between Institut Nationale Polytechnique de Toulouse France and School of Electrical Engineering and Informatics, Bandung Institute of Technology, Indonesia, in 2009. He is a researcher at Electrical Energy Conversion Research Laboratory, ITB. Since 2008, he is a lecturer at School of Electrical Engineering and Informatics ITB, Indonesia. His research interests include power electronics and electrical machinery. Dr. Tri Desmana Rachmildha can be contacted at School of Electrical Engineering and Informatics ITB, Jl. Ganesha 10 Bandung, Indonesia 40132 or at trides@konversi.ee.itb.ac.id and trides@gmail.com

Yanuarsyah Haroen was born in Indonesia in 1952. He received B.Eng degree in electrical engineering from Bandung Institute of Technology (ITB), Indonesia, in 1976. He received Diplôme Ingenieur, DEA/Master, and Docteur Ingenieur degrees from ENSEEIHT-INPT-France, in 1980, 1981, and 1983, respectively. Since 1999 he became a Professor. He is a lecturer at School of Electrical Engineering and Informatics ITB, Indonesia, since 1978. His research interests include electrical machinery, power electronics, renewable energy, and electrical traction applications. Prof. Dr. Yanuarsyah Haroen can be contacted at School of Electrical Engineering and Informatics ITB, Jl. Ganesha 10 Bandung, Indonesia 40132 or at yanuar@stei.itb.ac.id and yanuar@konversi.ee.itb.ac.id

Estiko Rijanto was born at Purbalingga-Indonesia in 1967. In 1987 he enrolled at Institut Teknologi Bandung (ITB) - Indonesia, and he pursued his B.Eng. under the Overseas Fellowship Program (OFP) IV scholarship from the Republic of Indonesia in 1988. He completed his B.Eng. degree at Tokyo University of Agriculture and Technology (TUAT), Tokyo - Japan in 1993. He received M. Eng. and Dr. Eng. degrees from the same university in 1995 and 1998, respectively. He has been conducting R&D activities at the Research Centre for Electrical Power and Mechatronics, the Indonesian Institute of Sciences (LIPI) in Bandung - Indonesia. In 2013, he was inaugurated the Research Professor on Applied Control Systems by LIPI. His research interests include control systems and their applications for power generations, power electronics, renewable energies, battery management systems, electric vehicles, robotics, and mechatronics. Prof. Dr. Estiko Rijanto can be contacted at estiko.rijanto@lipi.go.id and estikorijanto@gmail.com